

Light-Induced Hypoxia in Carbon Quantum Dots and Ultrahigh Photocatalytic Efficiency

Sanjit Mondal, Soumya Ranjan Das, Lipipuspa Sahoo, Sudipta Dutta, and Ujjal K. Gautam*



Cite This: <https://doi.org/10.1021/jacs.1c10636>



Read Online

ACCESS |



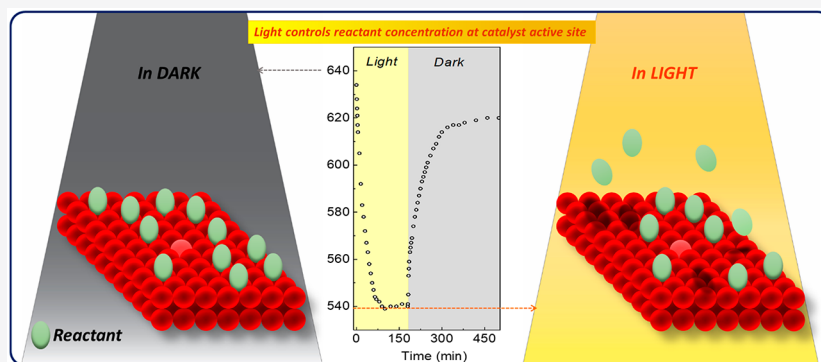
Metrics & More



Article Recommendations



Supporting Information



ABSTRACT: Carbon quantum dots (CQDs) represent a class of carbon materials exhibiting photoresponse and many potential applications. Here, we present a unique property that dissolved CQDs capture large amounts of molecular oxygen from the air, the quantity of which can be controlled by light irradiation. The O_2 content can be varied between a remarkable 1 wt % of the CQDs in the dark to nearly half of it under illumination, in a reversible manner. Moreover, O_2 depletion enhances away from the air–solution interface as the nearby CQDs quickly regain them from the air, creating a pronounced concentration gradient in the solution. We elucidate the role of the CQD functional groups and show that excitons generated under light are responsible for their tunable adsorbed-oxygen content. Because of O_2 enrichment, the photocatalytic efficiency of the CQDs toward oxidation of benzylamines in the air is the same as under oxygen flow and far higher than the existing photocatalysts. The findings should encourage the development of a new class of oxygen-enricher materials and air as a sustainable oxidant in chemical transformations.

INTRODUCTION

Increasing the adsorption of reactant molecules on the surface of a heterogeneous catalyst is necessary to attain high catalytic efficiencies for chemical transformations and energy harvesting applications. This is nonetheless rather difficult to achieve for gases such as O_2 having low solubility and diffusion rates in solutions.^{1,2} Even though presaturation or continuous gas purging can improve the reaction rates, the process becomes expensive and unfriendly for the industry. Moreover, under photocatalytic conditions, the adsorption–desorption equilibrium of the gases on the catalyst surface may significantly vary because of the modified electronic structure of the catalyst in the presence of the photoexcited electrons and holes.^{3,4} However, the effect of light on the concentration of O_2 or other reactants on a catalyst surface has remained poorly explored, hindering the development of highly active photocatalysts and the use of the ambient air as an inexpensive oxidizing reagent.

Semiconducting carbon quantum dots (CQDs), comprised of small functionalized graphene layers, are a class of light-responsive materials with potential applications in photocatalysis, electrocatalysis, solar hydrogen generation, and also

biomedical diagnosis and therapeutic approaches where the interactions of O_2 and graphene play a central role.^{5–10} Recently, while developing a rational strategy for a residue-free, large-scale production of carbon quantum dots using waste plastic (PE-CQDs), we serendipitously observed that the ability of water to dissolve and diffuse molecular oxygen increases significantly in their presence.¹¹ When a tiny PE-CQD concentration of ~0.1 wt % is used, the total oxygen content (TO) measures double that of pure water (320 μM) when the solution is exposed to air. The oxygen enrichment is reversible, shuttling between 640 and 95 μM in the air and N_2 atmosphere (Figure 1). It was further proposed that the O_2 enrichment ought to result in extraordinarily high efficiency for oxidation reactions while using PE-CQDs as photocatalysts,

Received: October 8, 2021

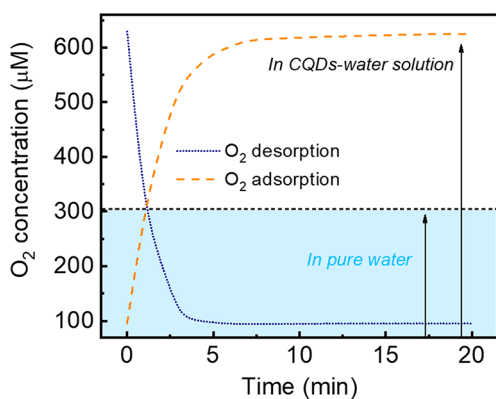


Figure 1. Temporal variation of total oxygen content in an aqueous solution of PE-CQDs (concentration ~ 1 wt %) during purging with nitrogen and subsequently during spontaneous oxygen uptake from the air by the nitrogen-saturated solution. The shaded region refers to the TO range similarly obtained in pure water.

though these have primarily been utilized for photoreduction reactions.^{12–16}

The findings inspire several scientific inquiries that can lead to molecular O_2 or ambient air being used as a sustainable oxidizing agent, such as the enrichment mechanism and the nature of involvement of the functional groups on PE-CQDs in oxygen enrichment. Moreover, because the PE-CQDs absorb visible light to generate excitons that can interact with the surface-adsorbed O_2 (to form superoxide radical anions, making the CQD transiently a positively charged entity) or may accept electrons from reactants or solvent, it is also essential to examine as to how and to what extent exposure to light influences the oxygen enrichment properties.^{17–20} Past theoretical studies on the interactions of oxygen with graphitic carbon have revealed their bonding possibilities from the hybridization of the O $2p$ orbitals and the bonding π orbital of graphene, further tunable by the presence of defects and surface functionalities.^{21–24} These studies, though, form the basis of understanding oxygen enrichment in PE-CQDs and have considered the carbon structures to be in a vacuum while understanding the behavior of PE-CQDs in water requires the consideration of a dielectric surrounding mimicking the experimental design.

Herein, we present the origin of high oxygen adsorption on the PE-CQDs and the extraordinary effect of light illumination mimicking photocatalytic conditions on their O_2 adsorption properties. The TO value of its aqueous solution exhibits a terse decrease in the presence of light from 640 to 540 μM due to the desorption of O_2 . The variation in TO is reversible and regains the original value once the illumination ceases. The rate of TO depletion and the depleted saturation values are depth-dependent due to the variations in the diffusion path length of molecular O_2 and CQDs from solution to air, yielding a remarkable TO gradient of ~ 4.5 $\mu M/cm$. Using density functional theory, we show that the $-CO$ and $-OH$ groups are responsible for stabilizing the O_2 molecules on PE-CQDs in the dark. However, if a PE-CQD acquires some charge under photocatalytic conditions due to the interactions of excitons with reactants, the O_2 to PE-CQD binding further attunes so that a fraction of the O_2 molecules desorb from the surface. In contrast, the binding of another fraction synergistically improves in the vicinity of the $-SO_3H$ groups. By taking photo-oxidation of benzylamine derivatives as an example, we

show that due to high oxygen content, the photocatalytic oxidation ability of the PE-CQDs is remarkably higher in ambient conditions and natural sunlight than the existing photocatalysts, including those containing noble metals that use harsh reaction conditions. The findings establish CQDs as a molecular O_2 enricher in solution, paving the way for air as a sustainable oxidant in reactions.

EXPERIMENTAL SECTION

Materials and Methods. More details are described in Note S1 of the Supporting Information.

Synthesis of PE-CQDs. The PE-CQDs were prepared by carbonization of polyethylene followed by its oxidation with $KMnO_4$ and H_2O_2 (for details see Note S1).¹¹ Briefly, 1 g of polyethylene (PE) was added to 60 mL of 18 M sulfuric acid and refluxed at ~ 150 $^\circ C$ for 1 h with constant stirring where the transparent PE sheets turned black. $KMnO_4$ solution (1 g in 20 mL of water) was added dropwise to the reaction mixture, followed by 1.5 mL of H_2O_2 , resulting in an orange-yellow solution of PE-CQDs. The solution was allowed to cool to room temperature and diluted by adding 60 mL of water. Thereafter, the PE-CQDs were repeatedly extracted with ethyl acetate in a separating funnel. The PE-CQDs–ethyl acetate solution was filtered through Na_2SO_4 to remove moisture and then evaporated by using a rotary evaporator to obtain the solid powder of PE-CQDs.

Measurement of Oxygen Content in the PE-CQD Solutions. The total oxygen content (TO) in pure water and an aqueous dispersion of PE-CQDs was measured at room temperature (25 – 27 $^\circ C$) by using noninvasive an Ocean Optics Neoflex-Kit-Probe.^{11,25} A linear calibration plot was ascertained in the required measurement range by using various ($N_2 + O_2$) gas mixtures. Prior to all measurements, the oxygen sensing kit was calibrated by using a two-point reading (20.9% O_2 in air and 0% O_2 in N_2). 60 mL of water containing 50 mg of the PE-CQDs (1 mg/1.2 mL) was taken in a 50 mL glass round-bottom flask (RBF, total capacity ~ 65 mL). The sensing patch was attached to the inner wall of the flask in such a way that it was completely submerged in the solution. The RBF was left open (neck radius 1.5 cm, opening area 7 cm^2) so that the PE-CQD solution was in contact with air to uptake O_2 or release dissolved O_2 . During the O_2 desorption measurements, the solution was kept still and N_2 gas was bubbled through the solution at a constant flow rate of 60–70 sccm. When the TO value did not decrease any further under the N_2 flow, the flow was stopped, and the solution was then used to measure oxygen uptake properties from the air. Under constant stirring at 300 rpm for faster homogenization, the TO values of this solution were recorded at regular intervals of time. The effect of light illumination on TO was measured by exposing the same PE-CQD solution to light of appropriate wavelength by using a Xe arc lamp (400 W, Newport, and appropriate cutoff filters). The distance between the RBF and Xe lamp was ~ 60 cm. TO data were recorded in 1, 3, or 5 min intervals depending on the rate of change. The oxygen sensing patch was covered from light for ~ 15 s before each measurement. When the TO values reached a minimum in the presence of light, the lamp was switched off, and the measurements were continued until the initial TO value was reached. The variation in data points is about 14–16 μM in the presence of light and 8–10 μM in the dark. Note that the variations in the TO values are stirring rate and air–solution surface area dependent.¹¹ Therefore, all measurement conditions were kept constant throughout the measurements.

Benzylamine Oxidation Using PE-CQDs. Selective photo-oxidation reactions of benzylamine and its derivatives were performed at room temperature (maintained at 32–33 $^\circ C$ with a water bath) under the necessary atmospheres (air, O_2 , or N_2) by using 0.5 mmol of BA in an RBF containing 15 mg of PE-CQDs in 30 mL of acetonitrile under either a Xe lamp (400 W, Newport attached with an aqueous IR filter) or direct sunlight (details in Note S2 and Figure S1). The yields of the benzylamine reactions were further confirmed by measuring the weight of the crude product after separating the

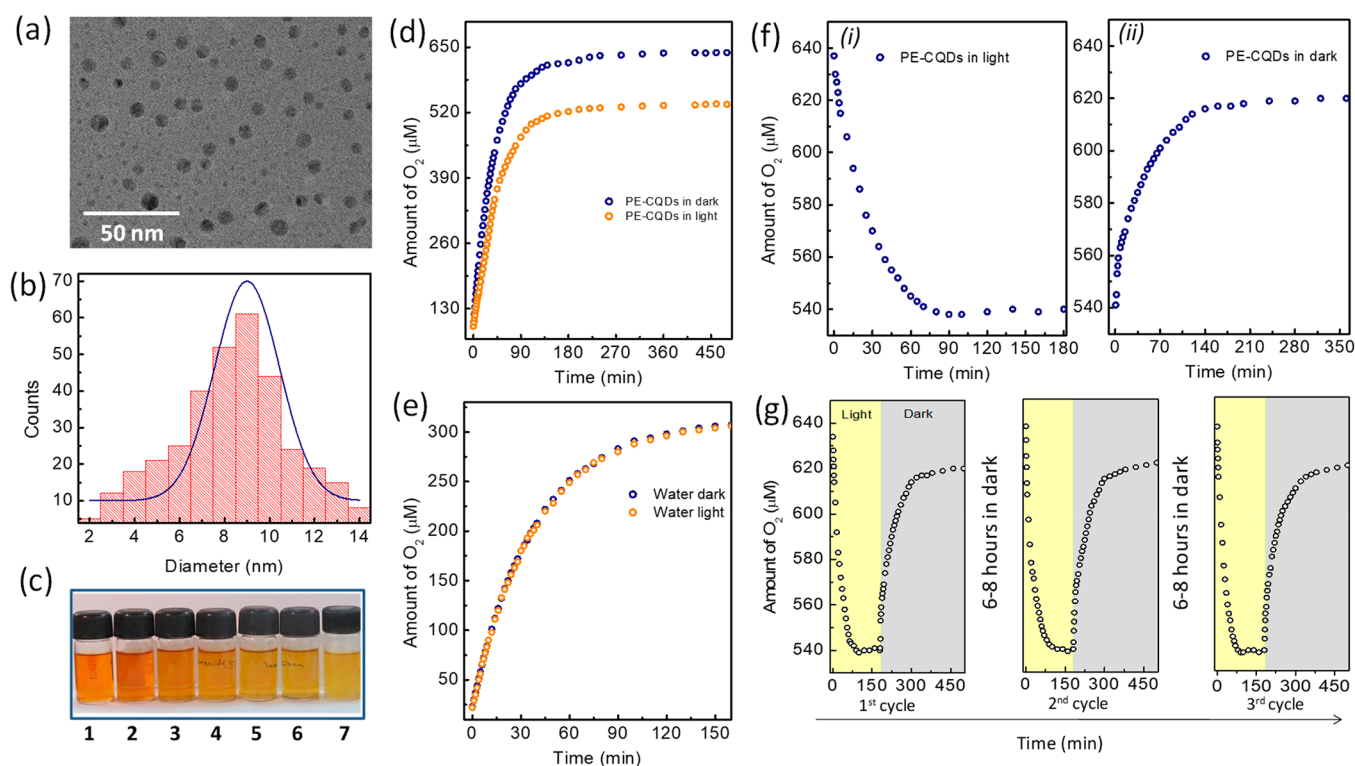


Figure 2. Three-year-old PE-CQDs. (a) TEM image and (b) particle size distribution. (c) Photograph of solutions of the PE-CQDs using different solvents (1 mg/2 mL), stable for several months: 1, water; 2, methanol; 3, ethanol; 4, ethyl acetate; 5, acetonitrile; 6, acetone; and 7, isopropyl alcohol. (d) Temporal variation in TO in a previously deoxygenated (by N_2 purging) aqueous PE-CQD solution (1 mg/1.2 mL) by spontaneous oxygen uptake from the air, in the dark, and under light, reaching saturated TO values of 640 and 540 μM , respectively. (e) Oxygen uptake in deoxygenated water in the dark and under light, reaching identical saturated TO values of 310 μM . (f) Temporal variation in TO values in the aqueous PE-CQDs solution under constant irradiation of light (i) and the reabsorption of O_2 in the dark (ii). (g) Three repeat cycles showing a decrease in TO values of the PE-CQD solution under light and O_2 reabsorption in the dark. Note that the time taken to regain the saturation TO value in air is quite long, 12–15 h (deviation in TO from mean value: ± 5 –8 μM).

CQDs by centrifugation repeatedly by adding several batches of acetonitrile. The isolated yield was obtained by using a neutral alumina column and hexane + 1% ethyl acetate as mobile phase. Note that the CQDs can be eluted by using methanol. Mineralization of the reactant molecules during photocatalysis was estimated by measuring CO and CO_2 formation using gas chromatography (Shimadzu GC 2014, FID detector), and the same was found to correspond to <1% of the reactants after 55 min of the reaction. The repeatability test was performed by performing the photocatalytic reaction again in the previously used solution by adding an equal amount of reactant molecules. Nuclear magnetic resonance spectroscopy (400 MHz Bruker Biospin Avance III FT-NMR spectrometer) was used to analyze the products of the photocatalytic oxidation reactions (NMR data are given in the Supporting Information).

Simulation Studies. Details are given in Note S3.

RESULTS AND DISCUSSION

The PE-CQDs form a transparent yellowish dispersion in water, which is stable for over three years without any remarkable changes in the properties. Transmission electron microscopic (TEM) imaging of the sample shows that the average size of the PE-CQDs is 8.5 nm, containing the graphitic lattice planes (Figure 2a,b and Figure S2). These contain C atoms attached to hydroxyl ($-\text{OH}$), carbonyl ($-\text{C}=\text{O}$), carboxyl ($-\text{COOH}$), and sulfonyl ($-\text{SO}_3\text{H}$) groups with a relative abundance in the range 8–15%.¹¹ We found that the Fourier transformed infrared (FT-IR) spectrum, X-ray diffraction pattern, UV–vis absorption, and photoluminescence spectrum of the old PE-CQDs powder remain

similar to a fresh sample (Figure S3), suggesting their chemically stable nature. Furthermore, the PE-CQDs are soluble in many solvents such as water, methanol, ethanol, ethyl acetate, acetonitrile, acetone, and isopropanol without precipitation for months to make them potentially useful in many catalytic applications (Figure 2c).

The measurements on the total oxygen content of an aqueous PE-CQDs solution were performed by using a typical concentration of 1 mg of PE-CQD/1.2 mL of water. The TO value of this solution decreases from $640 \pm 7 \mu\text{M}$ in the air to $\sim 95 \pm 5 \mu\text{M}$ under continuous bubbling of N_2 gas. Subsequently, when the N_2 flow is stopped, as seen in Figure 2d, oxygen diffuses again from the air into the solution to attain the initial saturation value. The initial rise in TO is rapid, reaching half of the saturation value within 25 min. It took much longer, ~ 125 min thereafter, to uptake the remaining half of the oxygen molecules. However, we found that the saturation value is significantly different when the uptake of O_2 from air occurred in the presence of light. As shown in Figure 2d, when the solution was irradiated with a 400 W Xe lamp, the saturation TO value became $540 \pm 8 \mu\text{M}$, nearly 100 μM less than the same in the absence of light. The contrast becomes apparent when compared with the same measurements performed in pure water wherein the saturation TO value remains $\sim 310 \pm 7 \mu\text{M}$ either in the presence or absence of light (Figure 2e). The observations gave rise to a belief that light, or probably the excitons generated by it, in the PE-CQDs offers a possibility to control the total oxygen content in water.

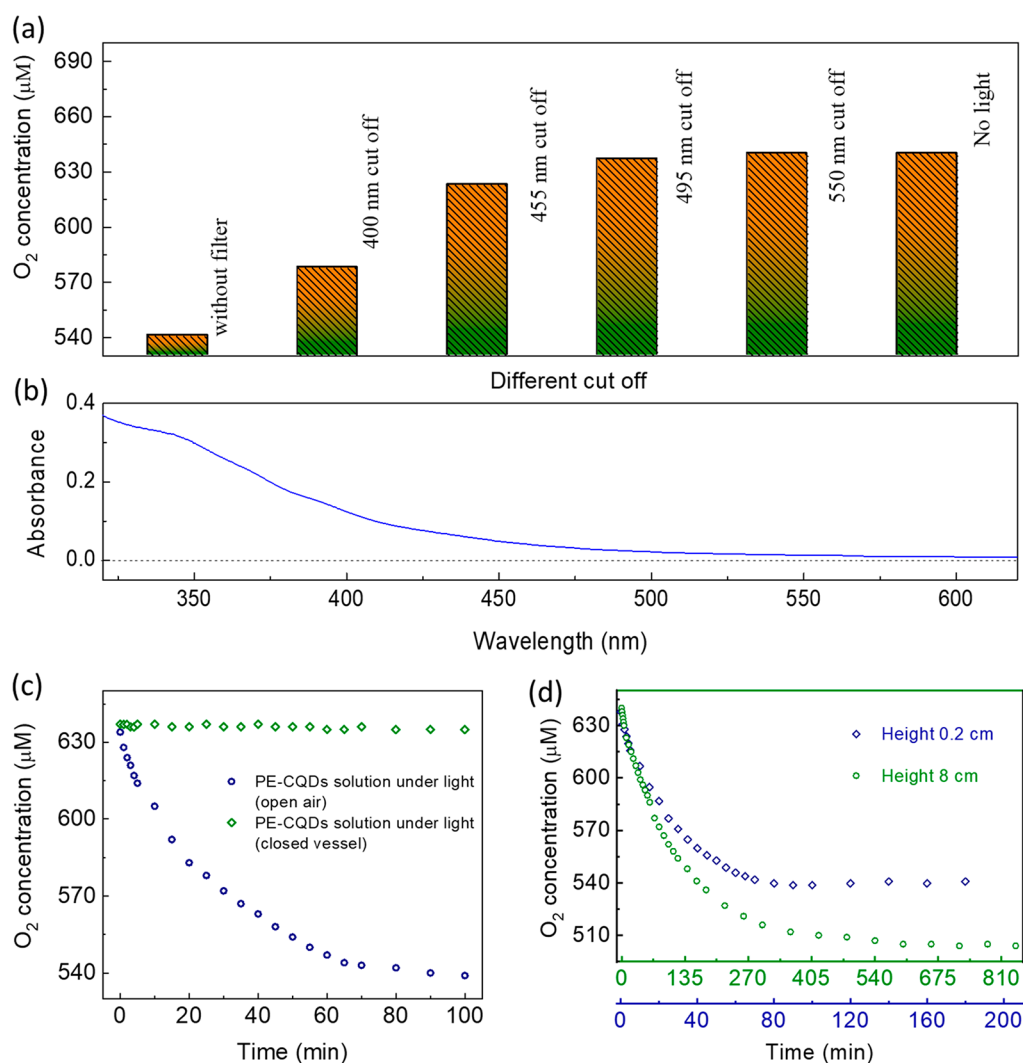


Figure 3. (a) TO values observed in the PE-CQD solution under constant irradiation of the light by using different cutoff filters. (b) UV-vis absorption spectrum of the PE-CQD solution closely matching the variation in TO values in (a). Comparison of temporal variations in TO values in the aqueous PE-CQD solution under constant irradiation of light (c) in an open and a closed vessel, (d) at two different depths from the solution-air interface: 0.2 and 8 cm in an open vessel (deviation in TO from mean value: ± 5 – $8 \mu\text{M}$).

To examine the effect of light on total oxygen content in greater detail, we have exposed the aqueous PE-CQD solution continuously to irradiation from a 400 W Xe lamp and measured the TO values in regular intervals, as shown in Figure 2f. The TO values exhibited a sharp drop initially within the first few minutes and continued to decline, though the variation became progressively slower until attaining a saturation value of $540 \pm 8 \mu\text{M}$ in 80 min. No further changes in the TO values were observed at this point, even upon prolonged light irradiation.

The changes in the oxygen content are reversible in nature, and the PE-CQD solution picks up oxygen again once the Xe lamp is switched off (Figure 2f). The TO values begin to increase, initially rapidly regaining 25% and 50% of the lost oxygen in about 10 and 45 min, respectively, and reach $\sim 620 \pm 8 \mu\text{M}$ in about 220 min. It takes another 10–12 h to reach the original TO value of $\sim 640 \pm 8 \mu\text{M}$. Figure 2g shows three successive cycles with similar variations in the presence and absence of light.

The origin of the variation in oxygen level in the PE-CQD solution was examined from the following controlled experi-

ments. It was found that the extent of variation in the TO values is dependent on the wavelength of the irradiating light. As seen in Figure 3a, the saturated TO values increased from $540 \mu\text{M}$ when exposed to the full spectrum of light to become 580, 625, and $640 \mu\text{M}$ upon using 400, 455, and 495 nm cutoff filters, respectively. The values did not change any further, as expected, by using a 550 nm cutoff filter. Noting that the dependence of the TO values closely matches the UV-vis absorption spectra of the PE-CQD solution (Figure 3b and Figure S3c) where the absorption onsets at $\sim 500 \text{ nm}$ and the fact that light irradiation makes a difference in the TO values only when PE-CQDs are present in water, and not in pure water, we attribute the variation in the oxygen content to the excitons generated in the PE-CQDs by light irradiation.

Furthermore, because the oxygen level reaches a depleted saturation value of $540 \mu\text{M}$ upon light irradiation, we have presumed the existence of an adsorption-desorption equilibrium on the PE-CQD surfaces; that is, the light induces desorption of the oxygen molecules, and subsequently the deficient CQD reabsorbs oxygen from the air. To confirm this hypothesis, first, the light irradiation experiment was repeated

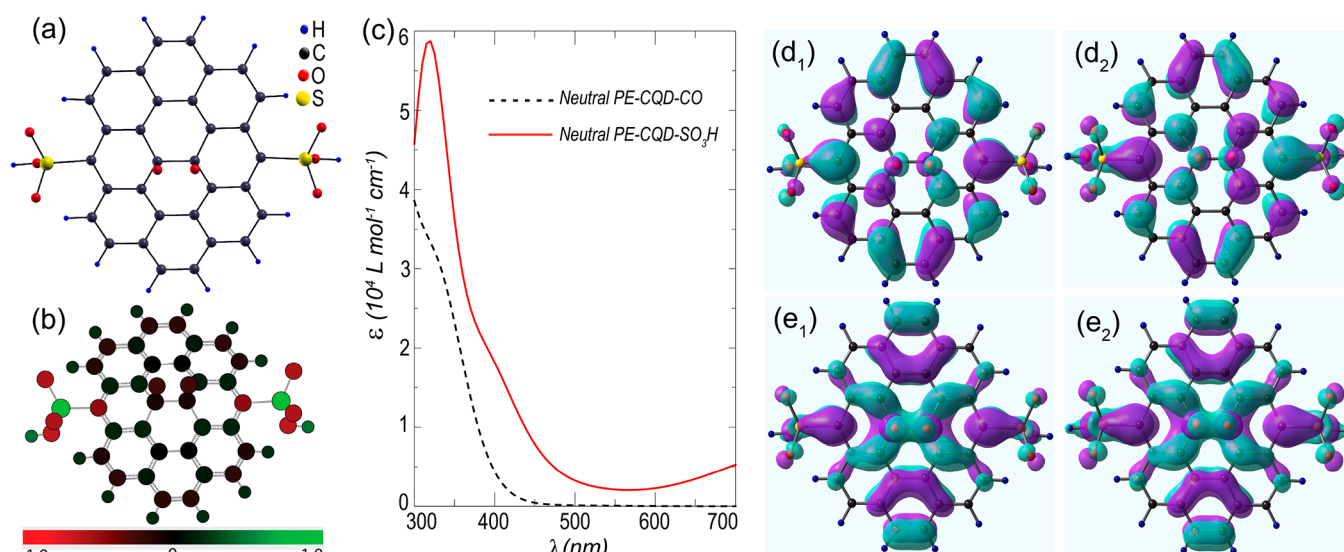


Figure 4. (a) Top view of the molecular structure of a zigzag-edge PE-CQD functionalized with two sulfonate groups, containing one adsorbed oxygen molecule. (b) The Mulliken electron density on each atom of the system in (a) is shown as per the relative color bar at the bottom. The structure is slightly tilted for a clearer view of all the atoms. (c) Theoretical UV-vis spectra of the neutral PE-CQD system functionalized with $-\text{C}=\text{O}$ and $-\text{SO}_3\text{H}$ groups. (d) and (e) denote the isosurfaces of HOMO and LUMO of the system, respectively (isovalue: 0.02). The subscripts 1 and 2 denote the neutral and negatively charged systems, respectively.

in a closed and completely filled vessel so that the PE-CQDs cannot get exposed to air. As seen in Figure 3c, no changes in the TO values were observed under light irradiation because even though the O_2 molecules were released from the PE-CQD surface, they could not escape and remained within the solution. Second, we have measured the TO level under light irradiation and open-air conditions at a different depth inside the vessel. In our previous study, we have demonstrated that oxygen enrichment becomes slower at larger depths. This is because the oxygen-deficient PE-CQDs must reach the solution surface to pick up oxygen from the air, or alternatively, if they adsorb O_2 from the surrounding water, oxygen from the air must diffuse a longer distance to reach the CQD surrounding, both processes needing a longer time at larger depth. Figure 3d shows the TO depletion profiles at 0.2 and 8 cm below the solution surface under Xe lamp irradiation. As expected, it took only 60 min to reach $\sim 90\%$ TO depletion at 0.2 cm but 250 min at 8 cm. Besides, because the uptake is slower at 8 cm, but the light-induced O_2 desorption rate is expected to remain similar, the depleted saturation TO value at 8 cm is $\sim 505 \mu\text{M}$, $35 \mu\text{M}$ less than the same at 0.2 cm, thereby implying a negative downward gradient of $4.5 \mu\text{M}/\text{cm}$ in the TO values inside the solution.

The light-irradiation experiments demonstrate that (i) the adsorbed oxygen content on the surface of a photoactive material can significantly vary in the presence of light, (ii) in the case of PE-CQDs the surface-bound oxygen contents are considerably high as compared to pure water, and (iii) a depth-dependent gradient in oxygen level may be created in a solution (containing a photoactive material) by using light.

Origin of High Oxygen Adsorption and Light-Induced Desorption. To theoretically study the light-modulated oxygen adsorption property of the PE-CQDs, we have taken a zigzag-edge planar CQD structure arranged in 10 six-membered rings as our model system (closely matching an actual PE-CQD, Note S4), as shown in Figure 4a and Figures S4–S7a. The edge carbons are saturated with hydrogen atoms. We have not considered the armchair edge PE-CQDs as it gets

distorted upon functionalization.²⁶ We have estimated the oxygen adsorption energies (E_A , Table 1) in the presence of

Table 1. Adsorption Energies of Neutral, Negatively, and Positively Charged PE-CQDs, Attached with Different Edge Functional Groups^a

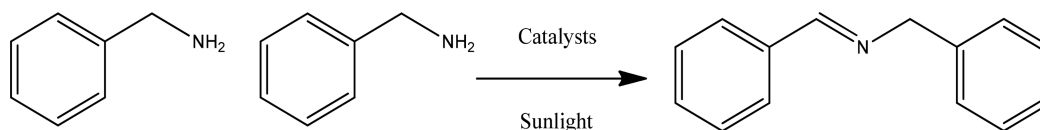
PE-CQD system (functional groups)	adsorption energy (E_A , eV)		
	neutral	negatively charged	positively charged
$-\text{SO}_3\text{H}$	1.31	5.82	-7.07
$-\text{COOH}$	1.36	0.18	-0.27
$-\text{OH}$	1.09	no adsorption	-0.27
$-\text{C}=\text{O}$	-0.5	no adsorption	-0.29
$-\text{SO}_3\text{H} + -\text{COOH}$	1.25	5.83	-7.17
$-\text{SO}_3\text{H} + -\text{OH}$	0.97	6.01	-7.45
$-\text{SO}_3\text{H} + -\text{CO}$	no adsorption	no adsorption	no adsorption

^aOne oxygen molecule is adsorbed on its surface. All the results are obtained in the presence of dielectric water solvent. The entry “no adsorption” refers to systems where we have not observed oxygen adsorption in PE-CQDs within the parameters of our theoretical optimization.

the various oxygen-containing functional groups (as observed from the XPS studies¹¹), that is, $-\text{SO}_3\text{H}$, $-\text{OH}$, $-\text{COOH}$, and $-\text{C}=\text{O}$, placed symmetrically along the edges of the quantum dots. This edge functionalization route was chosen as they are more reactive than the basal plane surface of PE-CQDs.²¹

Our theoretical investigation shows that the O_2 molecule preferentially adsorbs over the center of a PE-CQD, away from their reactive edges. The functionalized quantum dots get buckled on oxygen adsorption upon geometrical optimization (Figure 4b, Figures S6b and S7b). The adsorption of the O_2 molecule is favorable at the center of the C-surface by forming a four-membered ring (Figure 4a,b, Figures S6a,b and S7a,b) as in other carbon systems.^{21,27} In this configuration, a partial charge transfer takes place from the PE-CQD to oxygen (Figure 4b, Figures S6b and S7b), leading to an increased O–

Table 2. Optimization of Benzylamine Oxidation Reaction at Various Conditions*



entry	catalysts	environment	light	time (min)	# conversion (%)	selectivity (%)
1	PE-CQDs	air	sunlight	55	97	>99
2	PE-CQDs	air	Xe lamp	55	>98	>99
3 ^a	PE-CQDs	air	dark	55	<1	
4 ^b	PE-CQDs	air	dark	55	<1	
5 ^c	PE-CQDs	air	dark	55	<1	
6	PE-CQDs	O ₂	Xe lamp	55	>98	>99
7 ^d	PE-CQDs	N ₂	Xe lamp	55	70	>99
8 ^e	PE-CQDs	N ₂	Xe lamp	55	45	>99
9		air	sunlight	55	<1	
10 ^f	PE-CQDs	air	Xe lamp	55	32	>99
11 ^f	PE-CQDs	O ₂	Xe lamp	55	36	>99
12 ^f	PE-CQDs	N ₂	Xe lamp	55	8	>99
13	TiO ₂ -P25	air	Xe lamp	55	20	>99

*Reaction conditions: acetonitrile solutions (30 mL), containing substrates (0.5 mmol), photocatalyst (15 mg); a: room temperature (23–26 °C; b: 40 °C; c: 50 °C; d: reaction mixture was purged with N₂ and then PE-CQDs added into it. e: PE-CQDs were first added to the reaction mixture and then N₂ purged; f: reaction in a water medium (30 mL), keeping the other conditions identical. (Note: # conversion % indicates the percentage of imine in the crude product. The remaining % is the reactant. No other product was identified in the NMR spectra of the crude products. Selectivity is mentioned as >99% considering the possibility of a trace amount of other products that may not have been detected in NMR.)

O bond length (~1.55 Å) and a loss in the planarity of the C atoms beneath the O₂ molecule. We further inferred that the solvent dielectric medium in which the PE-CQDs are dispersed also stabilizes the oxygen molecule to promote a high O₂ uptake since the present E_A values are lower than those of graphitic quantum clusters in a vacuum.²¹

In the dark environment, we have observed that the adsorption is exothermic in the presence of the -C=O group due to an enhanced charge transfer but endothermic for the other functional groups, suggesting a weaker O₂ binding (Table 1). The theoretical UV-vis absorption spectrum for the PE-CQDs with two -C=O functional groups (Figure 4c, Figures S6c and S7c) closely matches with the experiment. Hence, the presence of the carbonyl group can be strongly linked to the unique oxygen enrichment in the PE-CQDs. Figure 4c also shows a close match of the theoretical UV-vis absorption spectrum for the -SO₃H-functionalized PE-CQDs with the experiment, despite being less stable than the carbonyl group-containing system. Notably, the presence of the -SO₃H group is unique in our PE-CQDs as compared to most other carbon dots as it originates from the sulfonation of the polyethylene backbone.¹¹ The highest occupied molecular orbital (HOMO) and the lowest unoccupied molecular orbital (LUMO) isosurface plots show that, in the presence of the weakly O₂ adsorbing functional groups (sulfonate groups in Figures 4d₁ and 4e₁), the excited-state wave functions are delocalized along the PE-CQD surface and the O₂ molecule. On the contrary, the frontier orbital isosurfaces for the carbonyl group-functionalized system show no contribution from the -C=O group (Figure S6d₁,e₁). Such a difference becomes crucial for an adsorption event taking place in the proximity of mixed functional groups. Consequently, oxygen adsorption does not occur when another functional group such as -SO₃H (Table 1) is attached to a PE-CQD containing a carbonyl group. However, the E_A values do not vary significantly in the presence of different combinations of other endothermic functional groups. Hence, even though the

carbonyl group-functionalized PE-CQD systems show enhanced stability on oxygen adsorption, we have chosen the sulfonate group for our subsequent investigation.

We further investigated the role of visible-light illumination to tailor oxygen adsorption of the PE-CQDs since excited electrons and holes are generated in this process. Consequently, the PE-CQDs under solar illumination can become either a negatively or positively charged entity by transferring one of the charge carriers to another species (such as H⁺, OH⁻, or molecular O₂) present in the solution. In such a charged system, the oxygen adsorption significantly varies from a neutral one depending on the functional group. Our calculations show that the endothermic adsorption energy increases 4-fold in a negatively charged PE-CQDs containing -SO₃H functional groups (Table 1). Figure 4d₂,e₂ shows the frontier orbital isosurfaces for the negatively charged system, similar to the neutral PE-CQDs, with identical charge transfer from carbon to oxygen. The oxygen molecule still appears to form a four-membered ring, but the high E_A suggests that oxygen molecules are loosely bound and likely to be present in the solution than near the system. Under light irradiation, oxygen desorbs from the PE-CQD surface to air when the experiment is conducted in an open vessel. Therefore, the TO value decreases in the presence of visible light to maintain the adsorption-desorption equilibrium.

Alternatively, the excited electron that goes from HOMO to LUMO can be captured by the oxygen molecule to form the superoxide anion radical (as experimentally inferred previously¹¹) and result in a positively charged PE-CQD. In this scenario, the adsorption energy becomes highly exothermic for most functional groups (Table 1). This favors a strong bond between the oxygen molecule and the PE-CQD surface, as observed from the frontier orbital isosurfaces of the positively charged systems in Figures S6d₂,e₂ and S7d₂,e₂. Moreover, the positively charged PE-CQD is stabilized by the surrounding dielectric water solvent, as evident from the exothermic nature of such a process.

Thus, the overall depletion of the TO content in the PE-CQD solution under light arises due to the interference from the excitons, which may be attributed either to the desorption of oxygen from the PE-CQD surface or to a very stronger adsorption so that O₂ becomes a part of the PE-CQDs and do not contribute to the TO measurement. However, in the experiments, since we observed no changes in the TO content under the closed conditions and light irradiation (Figure 3c), we conclude the desorption is the primary mechanism for the TO decrease.

Photocatalytic Oxidation of Benzylamine. The PE-CQDs were used as photocatalysts for the controlled oxidation of benzylamine (BA) and its derivatives to the corresponding imines by using the large number of O₂ molecules present on the PE-CQDs (Note S4) as the oxidant. The development of amine to imine transformation methodologies that are mild and green has gained attention because of their use in functional organic and medicinal compounds.^{28,29} Among these, photocatalytic oxidation is attractive due to its energy efficiency, leading to the development of many efficient photocatalysts.^{30–37}

The transformations were performed at room temperature in ambient air with excellent efficiencies (97%) with >99% selectivity within 55 min of sunlight irradiation (Table 2, entry 1). A similar performance was obtained by using a 400 W Xe lamp (Table 2, entry 2). The yield of the crude product is ~98%, and that of the isolated yield obtained is ~95%. The conversion efficiency of benzylamine as a function of the reaction time under the optimized conditions is shown in Figure S8. In contrast, the conversion efficiency is negligible in the dark in the presence of the PE-CQDs, at the room as well as elevated temperatures (Table 2, entries 3–5), signifying the photocatalytic nature of the reaction. The reaction yield in air and light was also negligible in the absence of the PE-CQDs (<1%, Table 2, entry 9), confirming its contribution as a photocatalyst.

Usually, O₂ purging is performed in this reaction to improve its kinetics significantly.^{38–41} This step can be avoided with the PE-CQDs without compromising on the reaction rates due to their intrinsic oxygen enrichment properties. When we purged O₂ during the reaction, the conversion efficiencies were nearly the same as that in air, i.e., ~63% and >98% (vs 58% and >98% in air, Table 2, entry 6) after 20 min and 1 h, respectively. On the contrary, the PE-CQDs were expected to perform this reaction even under an inert atmosphere since adsorbed oxygen cannot be completely displaced by N₂, even by prolonged purging (Figure 1).¹¹ To examine the influence of surface-adsorbed O₂, we performed the reaction by (i) purging N₂ in the solvent and then adding the O₂ saturated PE-CQDs kept in air and (ii) the reverse, i.e., by adding the PE-CQDs to the reaction mixture first and then purging it with N₂, assuming that the second reaction would be slower due to a reduced surface concentration of O₂. As anticipated, the conversion efficiencies were rather decent after 1 h, though they dropped to ~70% and 45% in the first and the second case (Table 2, entries 7 and 8), asserting that the surface-adsorbed O₂ is primarily responsible for the oxidation reaction.

However, since the TO measurements were performed in water and the photocatalytic reactions were performed in acetonitrile which is a better solvent for this reaction, we have also performed the reactions in water to verify the effect of TO on the oxidation reaction. The conversions in water are significantly low as compared to those in acetonitrile: ~32% in

ambient air and ~36% under O₂ purging conditions (Table 2, entries 10 and 11) after 55 min. Moreover, the conversion efficiency decreases drastically to ~8% from 32% under N₂ purged (Table 2, entry 12), confirming that the trend is very similar to the reaction performed in acetonitrile solvent.

The apparent quantum efficiency (AQE) under direct sunlight was estimated to be 35% for the BA oxidation reaction by considering all photons absorbed in the 300–500 nm range where the PE-CQDs absorb >95% of light (details in Note S5 and Figure S9a).⁴² The AQE was also estimated at various incident wavelengths (380, 400, 450, 500, and 550 nm) as shown in Figure S9b. It was found that the AQE profile mimics the UV–vis absorption spectrum of the CQDs; i.e., the AQE at $\lambda = 550$ nm is very small (~0.2%) and gradually increases to ~25% at $\lambda = 380$ nm. The AQE should be further higher at higher frequencies of the incident light, as the absorbance of the CQD solution also rises thereafter.

For comparison of the catalytic activities, we have also performed the reaction under similar conditions using benchmark commercial TiO₂ (P-25), where the conversion was a mere ~20% after 1 h (Table 2, entry 13). The catalytic reaction was performed for five consecutive runs, and the conversion efficiency was 92% (1 h light irradiation) at the end of the fifth cycle, suggesting high stability of the PE-CQDs (Figure 5a). The used PE-CQDs were characterized by various

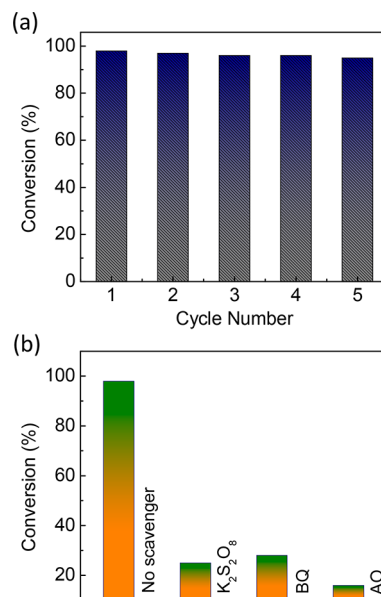
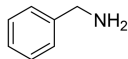
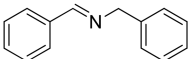
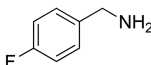
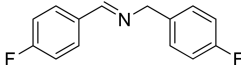
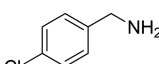
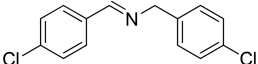
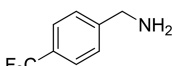
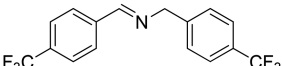
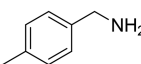
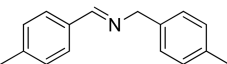
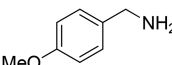
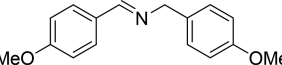
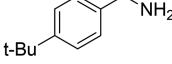
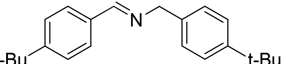
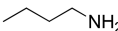
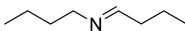


Figure 5. (a) Conversion efficiency during recycling of the PE-CQDs in five successive photocatalytic BA oxidation reactions. (b) Effect of different hole, electron, and radical scavengers in the conversion efficiency of the oxidation reaction.

techniques such as TEM, XRD, UV–vis, PL, and FT-IR spectroscopy, as described in Figures S10 and S11, to confirm their stability. The FT-IR spectra of the fresh and used CQDs revealed the preservation of various functionalization. Besides, oxygen harvesting properties and the dynamics of O₂ adsorption of the used CQDs remain similar to that of the fresh CQDs under both dark and light conditions, suggesting the high photostability of the CQDs (Figure S11c,d).

The performance of the PE-CQDs as photocatalyst under various gaseous environments exhibited a remarkable quality not observed in other photocatalysts. Earlier investigations

Table 3. Aerobic Oxidation of Different Substituted Amines with the PE-CQDs under Sunlight^a

Entry	Substrate	Product	Time	Conversion (%)	Selectivity (%)
1			55 min	>98	>99
2			75 min	94	>99
3			75 min	93	>99
4			75 min	92	>99
5			55 min	94	>99
6			55 min	90	>99
7			55 min	84	>99
8			2 h	0	-

^aReaction conditions: the reactions were performed in acetonitrile solutions (30 mL), containing substrates (0.5 mmol) and photocatalyst (15 mg) under the sunlight.

showed that the conversion is negligible when the reaction occurs in an inert atmosphere due to the absence of oxidants. By contrast, at least ~50% conversion was found under an inert atmosphere in our system. More importantly, the activity of the most state-of-the-art catalysts is significantly poorer in the open air as compared to an oxygen saturated atmosphere, requiring an additional oxygen flow while the activity of the PE-CQDs in the air is as high as under O₂ flow due to its intrinsic oxygen enrichment properties, thus offering a significantly simplified reactor-design possibility for large, industrial-scale utilization. Also, the reaction with other photocatalysts requires elevated temperatures to improve the kinetics.^{17,43–45} By considering such catalysts, including the ones with noble metals, the activity of the PE-CQDs under the mild conditions of room temperature and ambient air is still quite higher, as shown in the comparison (see Table S1).

The versatility of the PE-CQDs was examined by using para-substituted benzylamine with electron-donating (–CH₃, –OCH₃, *tert*-butyl) and electron-withdrawing (–F, –Cl, –CF₃) groups (Table 3). The electron-donating groups impart a somewhat better activity compared to the electron-withdrawing groups.

Mechanistic Insight. The excited electrons generated in the PE-CQDs by light irradiation activate the adsorbed O₂ molecules to induce the oxidation reaction.^{11,33,46,47} To develop further insight, several reactions were performed by using scavenger for excited electrons (K₂S₂O₈), holes (ammonium oxalate), and superoxide radical anions, O₂^{•–} (benzoquinone). The conversion drastically reduced by ~75% and ~82% respectively in the presence of K₂S₂O₈ and (NH₄)₂C₂O₄ to suggest a strong participation of both the excitons in the reaction (Figure S5b). The participation of the

O₂^{•–} radical anion was inferred from a slow (70%) reaction rate in the presence of benzoquinone.

Accordingly, we propose the following intermediate steps: (i) The excited electrons of the PE-CQDs transfer to the adsorbed O₂ to produce O₂^{•–}, *a*,^{47,48} as described in Scheme S1, Table S2, and Note S6. (ii) An adsorbed BA molecule becomes oxidized in the presence of a hole, yielding a benzylamine cation radical intermediate, *b*, and HOO•.^{31,49} The formation of intermediate *b* was confirmed by trapping it with TEMPO ((2,2,6,6-tetramethylpiperidin-1-yl)oxyl radical) and detecting the same by HRMS (Figure S12). (iii) Extraction of an H• radical by HOO• to produce benzyliminium ion, *c*, and H₂O₂ as a byproduct.⁵⁰ H₂O₂ formation was confirmed by KMnO₄ titration during the light irradiation (Figure S13); (iv) “*c*” couples with another neighboring BA molecule to give final product *d*, benzaldimine.¹⁷

CONCLUSIONS

In conclusion, we demonstrate that a carbon quantum dot can harvest large quantities of molecular oxygen from the air and adsorb them on its surface, aided by specific combinations of its surface functional groups. In addition, the concentration of adsorbed O₂ can be controlled by using an external light source so that a solution of CQDs can have different oxygen contents at different portions of the solution. The effect arises due to the modulation of charge transfer between the CQDs and the adsorbed O₂ molecules in the presence of light that generates excitons in the CQDs. The oxygen enrichment leads to profound photocatalytic efficiency for oxidative chemical transformations. The efficiency for controlled benzylamine oxidation is significantly higher than the existing photocatalysts, including those using expensive noble metals, an

oxygenated atmosphere, and harsh reaction conditions. Barely little is known about the concentration of gaseous reactants on a catalyst surface under photocatalytic conditions, and these findings will inspire such studies to explore the consequences on catalytic efficiencies. Moreover, the use of light and distance from the air–solution interface offers an unusual possibility of creating a landscape of varied oxygen contents in a solution that may offer new opportunities in chemical reactions.

■ ASSOCIATED CONTENT

SI Supporting Information

The Supporting Information is available free of charge at <https://pubs.acs.org/doi/10.1021/jacs.1c10636>.

Experimental methods, materials, details of synthesis, calculation details, theoretical methods, proposed reaction mechanism, comparison of activity, and figures and tables (PDF)

■ AUTHOR INFORMATION

Corresponding Author

Ujjal K. Gautam – Department of Chemical Sciences, Indian Institute of Science Education and Research (IISER)-Mohali, Mohali, SAS Nagar, Punjab 140306, India; orcid.org/0000-0002-0731-0429; Email: ujjalgautam@iisermohali.ac.in, ujjalgautam@gmail.com

Authors

Sanjit Mondal – Department of Chemical Sciences, Indian Institute of Science Education and Research (IISER)-Mohali, Mohali, SAS Nagar, Punjab 140306, India

Soumya Ranjan Das – Department of Physics, Indian Institute of Science Education and Research (IISER) Tirupati, Tirupati, Andhra Pradesh 517507, India; orcid.org/0000-0001-6160-1633

Lipipuspa Sahoo – Department of Chemical Sciences, Indian Institute of Science Education and Research (IISER)-Mohali, Mohali, SAS Nagar, Punjab 140306, India; orcid.org/0000-0002-7873-0252

Sudipta Dutta – Department of Physics and Center for Atomic, Molecular and Optical Sciences & Technologies, Indian Institute of Science Education and Research (IISER) Tirupati, Tirupati, Andhra Pradesh 517507, India; orcid.org/0000-0002-8944-813X

Complete contact information is available at: <https://pubs.acs.org/doi/10.1021/jacs.1c10636>

Notes

The authors declare no competing financial interest.

■ ACKNOWLEDGMENTS

This paper is dedicated to Professor Yoshio Bando on the occasion of his 75th birthday. S.M. is grateful to MHRD, India, for a senior research fellowship (SRF). L.S. thanks UGC (India) for SRF. Support from the Science and Engineering Research Board (SERB), India, under Grant CRG/2021/001420 is gratefully acknowledged. We acknowledge the facilities (TEM, XRD, NMR, PL, TCSPC) at IISER Mohali. S.R.D. and S.D. thank IISER Tirupati for Intramural Funding and SERB, Dept. of Science and Technology (DST), Govt. of India for research grant CRG/2021/001731. S.D. acknowledges National Supercomputing Mission (NSM) for providing computing resources of 'PARAM Brahma' at IISER Pune,

which is implemented by C-DAC and supported by the Ministry of Electronics and Information Technology (MeitY) and DST, Govt. of India.

■ REFERENCES

- (1) Chen, L.; Feng, X. Enhanced Catalytic Reaction at an Air–Liquid–Solid Triphase Interface. *Chem. Sci.* **2020**, *11* (12), 3124–3131.
- (2) Sheng, X.; Liu, Z.; Zeng, R.; Chen, L.; Feng, X.; Jiang, L. Enhanced Photocatalytic Reaction at Air–Liquid–Solid Joint Interfaces. *J. Am. Chem. Soc.* **2017**, *139* (36), 12402–12405.
- (3) Ollis, D. F. Kinetics of Liquid Phase Photocatalyzed Reactions: An Illuminating Approach. *J. Phys. Chem. B* **2005**, *109* (6), 2439–2444.
- (4) Nosaka, Y.; Nosaka, A. Y. Langmuir–Hinshelwood and Light-Intensity Dependence Analyses of Photocatalytic Oxidation Rates by Two-Dimensional-Ladder Kinetic Simulation. *J. Phys. Chem. C* **2018**, *122* (50), 28748–28756.
- (5) Lim, S. Y.; Shen, W.; Gao, Z. Carbon Quantum Dots and Their Applications. *Chem. Soc. Rev.* **2015**, *44* (1), 362–381.
- (6) Mondal, S.; Yucknovsky, A.; Akulov, K.; Ghorai, N.; Schwartz, T.; Ghosh, H. N.; Amdursky, N. Efficient Photosensitizing Capabilities and Ultrafast Carrier Dynamics of Doped Carbon Dots. *J. Am. Chem. Soc.* **2019**, *141* (38), 15413–15422.
- (7) Ge, J.; Lan, M.; Zhou, B.; Liu, W.; Guo, L.; Wang, H.; Jia, Q.; Niu, G.; Huang, X.; Zhou, H.; Meng, X.; Wang, P.; Lee, C.-S.; Zhang, W.; Han, X. A Graphene Quantum Dot Photodynamic Therapy Agent with High Singlet Oxygen Generation. *Nat. Commun.* **2014**, *5*, 4596.
- (8) Hutton, G. A. M.; Reuillard, B.; Martindale, B. C. M.; Caputo, C. A.; Lockwood, C. W. J.; Butt, J. N.; Reisner, E. Carbon Dots as Versatile Photosensitizers for Solar-Driven Catalysis with Redox Enzymes. *J. Am. Chem. Soc.* **2016**, *138* (S1), 16722–16730.
- (9) Shamsipur, M.; Barati, A.; Karami, S. Long-Wavelength, Multicolor, and White-Light Emitting Carbon-Based Dots: Achievements Made, Challenges Remaining, and Applications. *Carbon N. Y.* **2017**, *124*, 429–472.
- (10) Anand, A.; Unnikrishnan, B.; Wei, S.-C.; Chou, C. P.; Zhang, L.-Z.; Huang, C.-C. Graphene Oxide and Carbon Dots as Broad-Spectrum Antimicrobial Agents – a Minireview. *Nanoscale Horizons* **2019**, *4* (1), 117–137.
- (11) Mondal, S.; Karthik, P. E.; Sahoo, L.; Chatterjee, K.; Sathish, M.; Gautam, U. K. High and Reversible Oxygen Uptake in Carbon Dot Solutions Generated from Polyethylene Facilitating Reactant-Enhanced Solar Light Harvesting. *Nanoscale* **2020**, *12*, 10480.
- (12) Wang, Y.; Liu, X.; Han, X.; Godin, R.; Chen, J.; Zhou, W.; Jiang, C.; Thompson, J. F.; Mustafa, K. B.; Shevlin, S. A.; Durrant, J. R.; Guo, Z.; Tang, J. Unique Hole-Accepting Carbon-Dots Promoting Selective Carbon Dioxide Reduction Nearly 100% to Methanol by Pure Water. *Nat. Commun.* **2020**, *11* (1), 2531.
- (13) Yu, H.; Shi, R.; Zhao, Y.; Waterhouse, G. I. N.; Wu, L.-Z.; Tung, C.-H.; Zhang, T. Smart Utilization of Carbon Dots in Semiconductor Photocatalysis. *Adv. Mater.* **2016**, *28* (43), 9454–9477.
- (14) Fernando, K. A. S.; Sahu, S.; Liu, Y.; Lewis, W. K.; Gulians, E. A.; Jafariyan, A.; Wang, P.; Bunker, C. E.; Sun, Y.-P. Carbon Quantum Dots and Applications in Photocatalytic Energy Conversion. *ACS Appl. Mater. Interfaces* **2015**, *7* (16), 8363–8376.
- (15) Guo, S.; Zhao, S.; Wu, X.; Li, H.; Zhou, Y.; Zhu, C.; Yang, N.; Jiang, X.; Gao, J.; Bai, L.; Liu, Y.; Lifshitz, Y.; Lee, S.-T.; Kang, Z. A Co₃O₄-CDots-C₃N₄ Three Component Electrocatalyst Design Concept for Efficient and Tunable CO₂ Reduction to Syngas. *Nat. Commun.* **2017**, *8* (1), 1828.
- (16) Wu, J.; Ma, S.; Sun, J.; Gold, J. I.; Tiwary, C.; Kim, B.; Zhu, L.; Chopra, N.; Odeh, I. N.; Vajtai, R.; Yu, A. Z.; Luo, R.; Lou, J.; Ding, G.; Kenis, P. J. A.; Ajayan, P. M. A Metal-Free Electrocatalyst for Carbon Dioxide Reduction to Multi-Carbon Hydrocarbons and Oxygenates. *Nat. Commun.* **2016**, *7* (1), 13869.

- (17) Su, F.; Mathew, S. C.; Möhlmann, L.; Antonietti, M.; Wang, X.; Blechert, S. Aerobic Oxidative Coupling of Amines by Carbon Nitride Photocatalysis with Visible Light. *Angew. Chemie Int. Ed.* **2011**, *50* (3), 657–660.
- (18) Li, H.; Qin, F.; Yang, Z.; Cui, X.; Wang, J.; Zhang, L. New Reaction Pathway Induced by Plasmon for Selective Benzyl Alcohol Oxidation on BiOCl Possessing Oxygen Vacancies. *J. Am. Chem. Soc.* **2017**, *139* (9), 3513–3521.
- (19) Raza, F.; Park, J. H.; Lee, H.-R.; Kim, H.-I.; Jeon, S.-J.; Kim, J.-H. Visible-Light-Driven Oxidative Coupling Reactions of Amines by Photoactive WS₂ Nanosheets. *ACS Catal.* **2016**, *6* (5), 2754–2759.
- (20) Yuan, B.; Chong, R.; Zhang, B.; Li, J.; Liu, Y.; Li, C. Photocatalytic Aerobic Oxidation of Amines to Imines on BiVO₄ under Visible Light Irradiation. *Chem. Commun.* **2014**, *50* (98), 15593–15596.
- (21) Qi, X.; Song, W.; Shi, J. Density Functional Theory Study the Effects of Oxygen-Containing Functional Groups on Oxygen Molecules and Oxygen Atoms Adsorbed on Carbonaceous Materials. *PLoS One* **2017**, *12* (3), e0173864.
- (22) Bagican, F. R.; Winchester, A.; Ghosh, S.; Zhang, X.; Ma, L.; Wang, M.; Murakami, H.; Talapatra, S.; Vajtai, R.; Ajayan, P. M.; Kono, J.; Tonouchi, M.; Kawayama, I. Adsorption Energy of Oxygen Molecules on Graphene and Two-Dimensional Tungsten Disulfide. *Sci. Rep.* **2017**, *7* (1), 1774.
- (23) Lusk, M. T.; Wu, D. T.; Carr, L. D. Graphene Nanoengineering and the Inverse Stone-Thrower-Wales Defect. *Phys. Rev. B* **2010**, *81* (15), 155444.
- (24) Li, T.; Yarmoff, J. A. Defect-Induced Oxygen Adsorption on Graphene Films. *Surf. Sci.* **2018**, *675*, 70–77.
- (25) Kanan, M. W.; Nocera, D. G. In Situ Formation of an Oxygen-Evolving Catalyst in Neutral Water Containing Phosphate and Co²⁺. *Science* **2008**, *321* (5892), 1072–1075.
- (26) Cocchi, C.; Prezzi, D.; Ruini, A.; Caldas, M. J.; Molinari, E. Electronics and Optics of Graphene Nanoflakes: Edge Functionalization and Structural Distortions. *J. Phys. Chem. C* **2012**, *116* (33), 17328–17335.
- (27) Sorescu, D. C.; Jordan, K. D.; Avouris, P. Theoretical Study of Oxygen Adsorption on Graphite and the (8,0) Single-Walled Carbon Nanotube. *J. Phys. Chem. B* **2001**, *105* (45), 11227–11232.
- (28) Gnanaprakasam, B.; Zhang, J.; Milstein, D. Direct Synthesis of Imines from Alcohols and Amines with Liberation of H₂. *Angew. Chemie Int. Ed.* **2010**, *49* (8), 1468–1471.
- (29) Sun, H.; Su, F.-Z.; Ni, J.; Cao, Y.; He, H.-Y.; Fan, K.-N. Gold Supported on Hydroxyapatite as a Versatile Multifunctional Catalyst for the Direct Tandem Synthesis of Imines and Oximes. *Angew. Chemie Int. Ed.* **2009**, *48* (24), 4390–4393.
- (30) Mondal, S.; Sahoo, L.; Vaishnav, Y.; Mishra, S.; Roy, R. S.; Vinod, C. P.; De, A. K.; Gautam, U. K. Wavelength Dependent Luminescence Decay Kinetics in ‘Quantum-Confined’ g-C₃N₄ Nanosheets Exhibiting High Photocatalytic Efficiency upon Plasmonic Coupling. *J. Mater. Chem. A* **2020**, *8* (39), 20581–20592.
- (31) Li, S.; Li, G.; Ji, P.; Zhang, J.; Liu, S.; Zhang, J.; Chen, X. A Giant Mo/Ta/W Ternary Mixed-Addenda Polyoxometalate with Efficient Photocatalytic Activity for Primary Amine Coupling. *ACS Appl. Mater. Interfaces* **2019**, *11* (46), 43287–43293.
- (32) Garg, R.; Mondal, S.; Sahoo, L.; Vinod, C. P.; Gautam, U. K. Nanocrystalline Ag₃PO₄ for Sunlight- and Ambient Air-Driven Oxidation of Amines: High Photocatalytic Efficiency and a Facile Catalyst Regeneration Strategy. *ACS Appl. Mater. Interfaces* **2020**, *12* (26), 29324–29334.
- (33) Li, S.; Li, L.; Li, Y.; Dai, L.; Liu, C.; Liu, Y.; Li, J.; Lv, J.; Li, P.; Wang, B. Fully Conjugated Donor–Acceptor Covalent Organic Frameworks for Photocatalytic Oxidative Amine Coupling and Thioamide Cyclization. *ACS Catal.* **2020**, *10* (15), 8717–8726.
- (34) Zhao, F.-J.; Zhang, G.; Ju, Z.; Tan, Y.-X.; Yuan, D. The Combination of Charge and Energy Transfer Processes in MOFs for Efficient Photocatalytic Oxidative Coupling of Amines. *Inorg. Chem.* **2020**, *59* (5), 3297–3303.
- (35) Huang, Y.; Liu, C.; Li, M.; Li, H.; Li, Y.; Su, R.; Zhang, B. Photoimmobilized Ni Clusters Boost Photodehydrogenative Coupling of Amines to Imines via Enhanced Hydrogen Evolution Kinetics. *ACS Catal.* **2020**, *10* (6), 3904–3910.
- (36) Tu, X.; Wang, Q.; Zhang, F.; Lan, F.; Liu, H.; Li, R. CO₂-Triggered Reversible Phase Transfer of Graphene Quantum Dots for Visible Light-Promoted Amine Oxidation. *Nanoscale* **2020**, *12* (7), 4410–4417.
- (37) Mondal, S.; Sahoo, L.; Vinod, C. P.; Gautam, U. K. Facile Transfer of Excited Electrons in Au/SnS₂ Nanosheets for Efficient Solar-Driven Selective Organic Transformations. *Appl. Catal. B Environ.* **2021**, *286*, 119927.
- (38) Chen, H.; Liu, C.; Wang, M.; Zhang, C.; Luo, N.; Wang, Y.; Abroshan, H.; Li, G.; Wang, F. Visible Light Gold Nanocluster Photocatalyst: Selective Aerobic Oxidation of Amines to Imines. *ACS Catal.* **2017**, *7* (5), 3632–3638.
- (39) Furukawa, S.; Ohno, Y.; Shishido, T.; Teramura, K.; Tanaka, T. Selective Amine Oxidation Using Nb₂O₅ Photocatalyst and O₂. *ACS Catal.* **2011**, *1* (10), 1150–1153.
- (40) Wang, F.; He, X.; Sun, L.; Chen, J.; Wang, X.; Xu, J.; Han, X. Engineering an N-Doped TiO₂@N-Doped C Butterfly-like Nanostructure with Long-Lived Photo-Generated Carriers for Efficient Photocatalytic Selective Amine Oxidation. *J. Mater. Chem. A* **2018**, *6* (5), 2091–2099.
- (41) Han, A.; Zhang, H.; Chuah, G.-K.; Jaenicke, S. Influence of the Halide and Exposed Facets on the Visible-Light Photoactivity of Bismuth Oxyhalides for Selective Aerobic Oxidation of Primary Amines. *Appl. Catal. B Environ.* **2017**, *219*, 269–275.
- (42) Lingampalli, S. R.; Gautam, U. K.; Rao, C. N. R. Highly Efficient Photocatalytic Hydrogen Generation by Solution-Processed ZnO/Pt/CdS, ZnO/Pt/Cd_{1-x}Zn_xS and ZnO/Pt/CdS_{1-x}Sex Hybrid Nanostructures. *Energy Environ. Sci.* **2013**, *6* (12), 3589–3594.
- (43) Wang, M.; Wang, F.; Ma, J.; Li, M.; Zhang, Z.; Wang, Y.; Zhang, X.; Xu, J. Investigations on the Crystal Plane Effect of Ceria on Gold Catalysis in the Oxidative Dehydrogenation of Alcohols and Amines in the Liquid Phase. *Chem. Commun.* **2014**, *50* (3), 292–294.
- (44) Ye, J.; Ni, K.; Liu, J.; Chen, G.; Ikram, M.; Zhu, Y. Oxygen-Rich Carbon Quantum Dots as Catalysts for Selective Oxidation of Amines and Alcohols. *ChemCatChem* **2018**, *10* (1), 259–265.
- (45) Dhakshinamoorthy, A.; Alvaro, M.; Garcia, H. Aerobic Oxidation of Benzyl Amines to Benzyl Imines Catalyzed by Metal–Organic Framework Solids. *ChemCatChem* **2010**, *2* (11), 1438–1443.
- (46) Li, J.-Y.; Li, Y.-H.; Qi, M.-Y.; Lin, Q.; Tang, Z.-R.; Xu, Y.-J. Selective Organic Transformations over Cadmium Sulfide-Based Photocatalysts. *ACS Catal.* **2020**, *10* (11), 6262–6280.
- (47) Shi, J.; Zhang, J.; Liang, T.; Tan, D.; Tan, X.; Wan, Q.; Cheng, X.; Zhang, B.; Han, B.; Liu, L.; Zhang, F.; Chen, G. Bipyridyl-Containing Cadmium–Organic Frameworks for Efficient Photocatalytic Oxidation of Benzylamine. *ACS Appl. Mater. Interfaces* **2019**, *11* (34), 30953–30958.
- (48) He, H.; Li, Z.; Li, K.; Lei, G.; Guan, X.; Zhang, G.; Zhang, F.; Fan, X.; Peng, W.; Li, Y. Bifunctional Graphene-Based Metal-Free Catalysts for Oxidative Coupling of Amines. *ACS Appl. Mater. Interfaces* **2019**, *11* (35), 31844–31850.
- (49) Mao, C.; Cheng, H.; Tian, H.; Li, H.; Xiao, W.-J.; Xu, H.; Zhao, J.; Zhang, L. Visible Light Driven Selective Oxidation of Amines to Imines with BiOCl: Does Oxygen Vacancy Concentration Matter? *Appl. Catal. B Environ.* **2018**, *228*, 87–96.
- (50) Naya, S.; Kimura, K.; Tada, H. One-Step Selective Aerobic Oxidation of Amines to Imines by Gold Nanoparticle-Loaded Rutile Titanium(IV) Oxide Plasmon Photocatalyst. *ACS Catal.* **2013**, *3* (1), 10–13.